January, 1984]   © 1984 The Chemical Society of Japan   Bull. Chem. Soc. Jpn., 57, 179—183 (1984)   179

Molecular Motion and Phase Transitions in 2-Methyl-2-nitropropane as Studied by Proton Magnetic Resonance and Relaxation

Tooru Hasebe, Nobuo Nakamura,† and Hideaki Chihara*,†
Department of Chemistry, Faculty of Education, Fukushima University, Matsukawa-machi, Fukushima 960-12
†*Department of Chemistry, Faculty of Science, Osaka University, Toyonaka, Osaka 560*

(Received August 31, 1983)

Proton spin-lattice relaxation times (T_1 and $T_{1\rho}$) were measured in solid and liquid phases of 2-methyl-2-nitropropane. In the lowest temperature solid phase (Phase III) a broad, asymmetric minimum in T_1 as well as a large reduction in the second moment was observed due to the coupled reorientations of methyl and *t*-butyl groups. The analyses of the T_1 and $T_{1\rho}$ in Phase III gave the activation parameters $E_a=14.6\pm0.2$ kJ mol^{-1} and $\tau_0=(6.45\pm0.10)\times10^{-14}$ s for the methyl reorientation and $E_a=15.1\pm0.3$ kJ mol^{-1} and $\tau_0=(1.35\pm0.10)\times10^{-13}$ s for *t*-butyl reorientation. In Phase II, the T_1 is governed by the *t*-butyl reorientation with the activation parameters $E_a=15.3\pm0.1$ kJ mol^{-1} and $\tau_0=(5.85\pm0.10)\times10^{-14}$ s. In the low temperature region of the highest temperature plastic phase (Phase I) the molecular overall reorientation governs the T_1 and the molecular translational self-diffusion becomes the dominant relaxation mechanism near melting point. The $T_{1\rho}$ results were analyzed with the isotropic translational diffusion model and the activation parameters were determined to be $E_a=46.5\pm0.9$ kJ mol^{-1} and $\tau_0=(4.6\pm1.8)\times10^{-15}$ s. The mean jump time of the molecule at the melting point, 6×10^{-7} s, is slightly longer than those in other plastic crystals. The activation energy for the translational diffusion is 9.7 ± 1.5 kJ mol^{-1} in the liquid phase.

t-Butyl compounds $(CH_3)_3CX$ (where X=Cl, Br, NO_2, and CN) are globular molecules with relatively large electric dipole moments[1,2] and they commonly exist in three solid phases which are named Phase I, Phase II, and Phase III in the decreasing order of temperature. The highest temperature phase, Phase I, of these compounds except $(CH_3)_3CCN$ is a plastic crystal. Although the unit cell of the most plastic crystals has a high symmetry like fcc, hcp, and bcc, Phase I of 2-methyl-2-nitropropane ($(CH_3)_3CNO_2$) belongs to an orthorhombic system with two molecules in the unit cell. This phase exists between the melting point (299.2 K) and 260.1 K. The intermediate phase, Phase II, that appears between 260.1 and 215.3 K and the lowest temperature phase (Phase III) below 215.3 K are both triclinic.[3] Structure and properties of solid $(CH_3)_3CNO_2$ have been studied by many experimental methods.[2-13] The molecular motions in solid $(CH_3)_3CNO_2$ were examined by dielectric measurement,[9-11] pulsed NMR method[12] and quasi-elastic neutron scattering method.[13] Mazur and Nosel[12] measured the proton T_1 at 25.5 MHz from about 150 K to the melting point and derived the activaion energy for methyl reorientation about its C_3 axis, 15.5 ± 0.3 kJ mol^{-1}.

We measured proton magnetic resonance and relaxation (T_1 and $T_{1\rho}$) on the liquid and crystalline phases of $(CH_3)_3CNO_2$. The present paper reports its results and their interpretation in relation to the molecular motion and the phase transitions.

Experimental

2-Methyl-2-nitropropane obtained from Aldrich Chemical Co., Inc. was purified by a preparative gas chromatograph, followed by dehydration using Molecular Sieve 4A, vacuum distillation, and degassing by usual freeze-pump-thaw technique. The specimen was sealed under vacuum in a glass ampule of the outside diameter of 10 mm. The purity of the specimen was estimated to be higher than 99.87 mol per cent by a gas chromatographic analysis.

The melting point and the two transition points of this specimen were determined to be 298.7 ± 0.3, 260.1 ± 0.3, and 216.1 ± 0.3 K, respectively by differential thermal analysis (DTA).

The line-shape of ^{1}H-NMR was measured as a function of temperature between 77 and 260.1 K at 12.1 MHz using a Robinson-type spectrometer. The proton relaxation times in the laboratory frame, T_1, and in the rotating frame, $T_{1\rho}$, were measured by the use of Bruker CXP 4—60 MHz pulsed NMR spectrometer. T_1 was measured at 10.0 MHz and 15.0 MHz by the saturation recovery method $\{(\pi/2)_{\mathrm{comb}}-\tau-\pi/2$ pulse sequences$\}$ for the liquid and the plastic phase (Phase I), and by the inversion recovery method ($\pi-\tau-\pi/2$ pulse sequences) for Phase II and Phase III.

The magnetization recovered exponentially in the whole temperature range of the measurements. $T_{1\rho}$ was measured at 15.0 MHz with a rotating rf magnetic field (H_1) of 7.0 and 3.0 G†† (also with $H_1=2.0$ and $H_1=10.0$ G for Phase I) by the spin-locking method. Generally, T_1 and $T_{1\rho}$ measurements were carried out between 100 K and the melting point but T_1 at 10 MHz was measured up to 320 K.

The temperature was measured with a Chromel-P/Constantan thermocouple** and was controlled to within 0.1 K.

Experimental Results and Their Analysis

Line-shape. The derivative of the proton resonance line together with its integrated line-shape in the solid phases at a few selected temperatures are shown in Fig. 1. The line-shape at 84 K corresponds to a typical three proton system in the rigid lattice indicating that rotational motion of the methyl and the *t*-butyl groups are frozen at this temperature, whereas those at 173.2 and 225.5 K show that some large amplitude motions of molecules are excited at these temperatures.

The second moment of the absorption line at each temperature was calculated, corrected for the modulation width, and given in Fig. 2. One sees in this figure that the second moment decreases sharply

---

†† 1 G=10^{-4} T.

** This thermocouple with its temperature scale was kindly donated by Chemical Thermodynamics Laboratory, Faculty of Science, Osaka University.

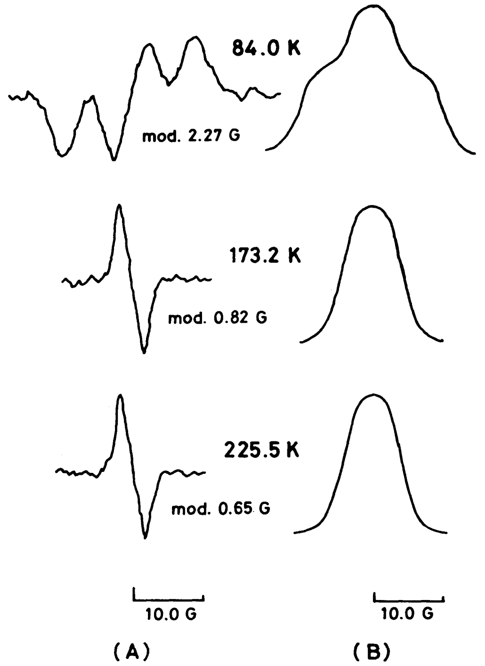

Fig. 1. Observed line shapes (A) and its integrated line shapes (B) at selected temperatures. The 'mod.' denotes modulation width of magnetic field.

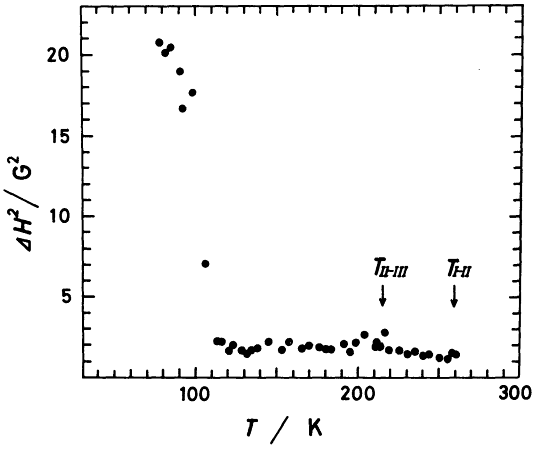

Fig. 2. Temperature dependence of the second moment.

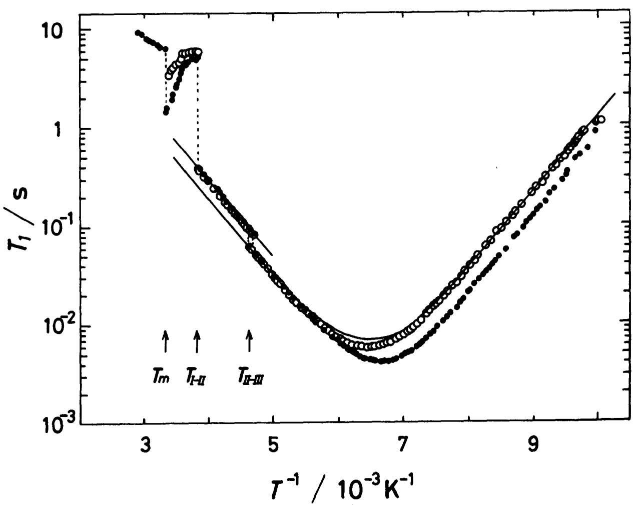

Fig. 3. Temperature dependence of spin-lattice relaxation times at 10 MHz (●) and 15 MHz (○).

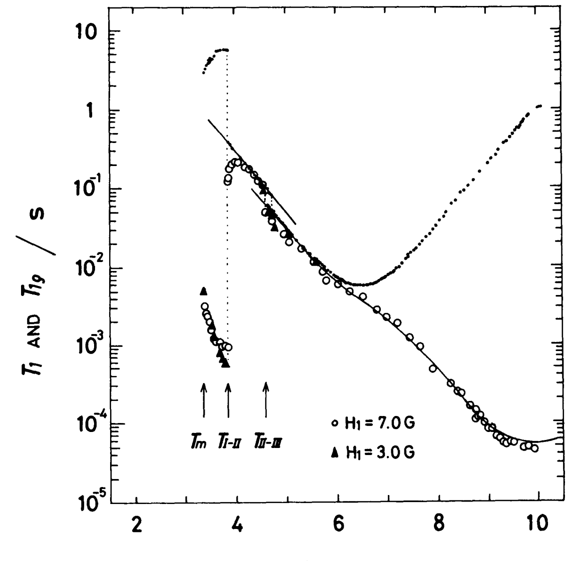

Fig. 4. Temperature dependences of the T_1(●) and the $T_{1\rho}$ at 15 MHz for rotating magnetic rf field of 7.0 G (○) and 3.0 G (▲).

between 80 and 110 K from 21 G^2 to 1.9 G^2. The intramethyl second moment calculated for a rigid lattice in a polycrystalline sample is 22.4 G^2, if the usual interproton distance, 0.178 nm, is used. The dipolar interaction between the methyl groups within one molecule contributes to the second moment by 1.8 G^2 which is based upon the tetrahedral and the staggered conformation of methyl groups in the molecule. Therefore, we obtain a value of 24.2 G^2 for the limiting low-temperature second moment without including the intermolecuar contribution.

If the methyl and the *t*-butyl groups rotate simultaneously, the intramethyl group second moment is reduced to 0.6 G^2 corresponding to the reduction factor 0.026.[14] The intermethyl second moment in one molecule becomes a quarter of 1.8 G^2. Therefore the concurrent reorientation of methyl groups about its C_3 axis and about the C_3' axis (C(Me)-C bond) causes the motional narrowing below 100 K in Phase III. Second moments of similar magnitude have been reported for a number of other compounds[15–19] containing *t*-butyl groups. Above 216 K, which is the phase transition point from Phase III to Phase II, the second moment further decreases gradually until the transition into Phase I occurs at 260.1 K, beyond which temperature the resonance line becomes narrower than the modulation width.

Spin-lattice Relaxation Times (T_2 and $T_{1\rho}$). Figure 3 shows the temperature dependence of the T_1 at 10 and 15 MHz in different phases of $(CH_3)_3CNO_2$. Discontinuities in the T_1 were observed at 298, 260, and 216 K due to the first order phase transitions. Among these discontinuities only the T_1 at the phase transition between Phase III and Phase II (216 K) showed a significant thermal hysteresis. The dielectric permitivity[9] in solid $(CH_3)_3CNO$ also showed a similar hysteresis at this phase transition.

The rotating frame relaxation times, $T_{1\rho}$, at the spin-locking field intensity (H_1) of 7.0 and 3.0 G together with the T_1 at 15 MHz are shown in Fig. 4. Discontinuity is also seen in the $T_{1\rho}$ at each transition point.

Relaxation in Phase III: In Phase III, a broad, slightly asymmetric minimum in the T_1 was observed. The minimum value was 4.2±0.2 ms at 149.3 K and 10 MHz, and 5.6±0.2 ms at 153.8 K and 15 MHz. These values are consistent with the results by Mazur and Nosel[12] at 25.5 MHz, *i.e.* 11.5 ms at 170.9 K. As was discussed in the preceding section, we infer that the motion responsible for the relaxation in Phase III is the simultaneous excitation of the C_3- and the C_3'-rotations. In this case we obtain the expression for T_1 as follows,

$$1/T_1 = (1/T_1)_{\text{intra}} + (1/T_1)_{\text{inter}} + (1/T_1)_{\text{intermol}}, \tag{1}$$

where 'intra' and 'inter' denote intramethyl and intermethyl (intramolecular) contributions to the T_1, respectively, and 'intermol' denotes intermolecular contribution to the T_1. However, since the intermolecular contribution to the T_1 is very difficult to estimate accurately when the molecular motion involves different types of reorientations and since this contribution is expected to be small compared with other contributions, we ignore it in the following analysis. The relaxation rate for dipolar interaction within the molecule undergoing C_3- and C_3'-rotations is given by

$$(1/T_1)_{\text{intra}} = (\gamma^4\hbar^2/60r^6)\{8B(\tau_{\text{m}}) + 8B(\tau_{\text{M}}) + 19B(\tau_{\text{c}})\}, \tag{2}$$

where r is the interproton distance in a methyl group, γ is the gyromagnetic ratio, τ_{m} and τ_{M} are the correlation times for C_3- and C_3'-rotations, respectively, and τ_{c} is defined by

$$1/\tau_{\text{c}} = 1/\tau_{\text{m}} + 1/\tau_{\text{M}}. \tag{3}$$

Here we used an approximation that C_3- and C_3'-rotations are mutually independent and ignored any correlation between these motions.[20,21]. The spectral density function $B(\tau)$ has the form

$$B(\tau) = \tau/(1+\omega^2\tau^2) + 4\tau/(1+4\omega^2\tau^2), \tag{4}$$

where ω is the Larmor frequency. The intermethyl contribution to the T_1 in the presence of the *t*-butyl reorientation is significantly large. In order to calculate this contribution, we assumed that the three protons in each methyl group reside at the center of the three proton system set. We can then calculate the relaxation rate due to the dipolar interaction between these hypothetical methyl groups as

$$(1/T_1)_{\text{inter}} = (27\,\gamma^4\hbar^2/20\,l^6)\text{B}(\tau_{\text{M}}), \tag{5}$$

where l is the distance between the centers of the methyl groups in a *t*-butyl group. The relaxation rate; $1/T_1$, is the sum of Eqs. 2 and 5;

$$1/T_1 = (2\,\gamma^4\hbar^2/15\,r^6)\{B(\tau_{\text{m}}) + B(\tau_{\text{M}})\} + (19\,\gamma^4\hbar^2/60\,r^6)B(\tau_{\text{c}}) + (27\,\gamma^4\hbar^2/20\,l^6)B(\tau_{\text{M}}). \tag{6}$$

Under the same assumption for the molecular motion as in the calculation of T_1 we calculated the $T_{1\rho}$, in the weak collision limit[22] as

$$1/T_{1\rho} = (\gamma^4\hbar^2/15\,r^6)\{G(\tau_{\text{m}}) + G(\tau_{\text{M}})\} + (19\,\gamma_4\hbar^2/120\,r^6)G(\tau_{\text{c}}) + (27\,\gamma^4\hbar^2/40\,l^6)G(\tau_{\text{M}}), \tag{7}$$

where $G(\tau)$ is the spectral density function,

$$G(\tau) = 5\,\tau/(1+\omega^2\tau^2) + 2\,\tau/(1+4\omega^2\tau^2) + 3\,\tau/(1+4\omega_1{}^2\tau^2), \tag{8}$$

and $\omega_1 = \gamma H_1$.

Activation parameters for these two types of motions were obtaind by fitting the data of Fig. 3 to Eq. 7 using r=0.178 nm and l=0.310 nm, and by assuming the Arrhenius equation for the temperature dependence of the correlation time for each of C_3-rotation and C_3'-rotation,

$$\tau = \tau_0 \exp(E_{\text{a}}/RT),$$

where τ_0 is the pre-exponential factor and E_{a} the activation energy. Here we used a following assumption: The straight line portion of the T_1 curve in the temperature region below the temperature of T_1(min) is mainly governed by the methyl reorientation and T_1 on the high temperature side of the T_1(min) by the *t*-butyl reorientation. The activation parameters thus obtained for the methyl reorientation and the *t*-butyl reorientation are tabulated in Table 1 and the T_1 reproduced with these parameters is shown in Fig. 3 by the solid line. The minimum value (6.7 ms at 154 K at 15 MHz) of the theoretical T_1 is somewhat larger than that of the observed T_1. The descrepancy is due to the simple nature of our theoretical model in which cross correlation effect of methyl and *t*-butyl group reorientation as well as intermolecular dipolar contribution to the T_1 were ignored. The solid line in Fig. 4 is the calculated $T_{1\rho}$ using Eq. 7 and the activation parameters obtained from the analysis of the T_1, data. The theoretical $T_{1\rho}$ in Fig. 4 is in reasonable agreement with the experimental $T_{1\rho}$. The minimum value of the calculated $T_{1\rho}$ is 54 µs which occurs at 100 K.

Similarity in the activation parameters for the two motions gives the broad minimum instead of a reported double minimum of the T_1 responsible for each of these motions.

Relaxation in Phase II: The T_1 jumps from 65 ms to 95 ms at the transition point, $T_{\text{II-III}}$, and then increases

TABLE 1. ACTIVATION PARAMETERS (E_{a} and τ_0) OBTAINED IN THIS STUDY FOR THE VARIOUS MOTIONS IN $(CH_3)_3CNO_2$

	Motion	E_{a}/kJ mol^{-1}	τ_0/s
Phase III	Methyl reorientation	14.6±0.2	$(6.45\pm0.10)\times10^{-14}$
	t-Butyl reorientation	15.1±0.3	$(1.35\pm0.10)\times10^{-13}$
Phase II	*t*-Butyl reorientation	15.3±0.1	$(5.85\pm0.10)\times10^{-14}$
Phase I	Translational diffusion	46.5±0.9	$(4.6\pm1.8)\times10^{-15}$
Liquid	Translational diffusion	9.7±1.5	

monotonously in Phase II with increasing temperature as is seen in Fig. 3. The $T_{1\rho}$ shows a similar jump in T_1 at $T_{\text{II-III}}$ but assumes a maximum value of 200±20 ms at 250 K, and then decreases with increasing temperature in Phase II. The decrease in the $T_{1\rho}$ above 250 K is due to the onset of an additional mode of molecular motion, probably the overall molecular tumbling. The activation energy obtained from the slope of log T_1 against reciprocal temperature below 250 K in Phase II is 15.3±0.1 kJ mol^{-1}. It agrees well with the E_a for the *t*-butyl reorientation in Phase III and gives support to the interpretation that the molecular motion governing the T_1 below 250 K is C_3'-rotation. As the change in the unit cell volume on going from Phase III to Phase II must be very small, considering the change of the second moment value (0.5 G^2), we can infer that the magnitude of intermolecular dipolar interaction does not change significantly. Hence we fitted the T_1 data in Phase II to Eq. 6 using the same E_a and the same molecular constants as in Phase III to estimate τ_0 for C_3'-rotation in Phase II. We obtained the τ_0 value of $(5.85\pm0.10)\times10^{-14}$ s which is shown in Table 1. At the transition point, $T_{\text{II-III}}$ (216.1 K), the correlation time for the *t*-butyl reorientation is changed discontinuously from 6.1×10^{-10} s to 3.0×10^{-10} s. It is interesting to see that the rate of C_3'-rotation increases by a factor of two at the transition from Phase III to Phase II, whereas the activation energy controlling this mode does not undergo any significant change. For Phase II, a study[13)] of quasi-elastic broadening in neutron scattering (QENS) led to the correlation time of about 1.6×10^{-12} s at 237 K for the 120° jump model for *t*-butyl group, which is larger than $\tau_c=1.4\times10^{-10}$ s at the same temperature deduced by using E_a and τ_0 in Table 1 by a factor of 100. It is hardly conceivable that the τ_c from NMR has such a large error since our value is consistent also with the narrowing condition. Thus, in Phase III, the *t*-butyl rotation has $\tau_c=1.0\times10^{-5}$ s at 100 K where the motional narrowing occurs. A difference by a factor of 100 means that the narrowing would occur when τ_c is as small as 10^{-7} s, which does not seem plausible. A similar discrepancy has been recognized in the solid phase of $(CH_3)_3CCl$: NMR measurements[23)] reported the correlation time of the order of 10^{-8} s for *t*-butyl reorientation, whereas QENS measurements[24)] reported the correlation time of the order of 10^{-12} s.

At the transition point, $T_{\text{I-II}}$ (260.1 K), a jump in $T_{1\rho}$ by a factor of 100 and the corresponding jump in T_1 by a factor of 10 were observed as seen in Figs. 3 and 4. The correlation time of C_3'-rotation in Phase II is 6.9×10^{-11} s at $T_{\text{I-II}}$. This value is much smaller than that $(4.3\times10^{-9}$ s$)$[23)] at the corresponding transition point of $(CH_3)_3CCl$. It was pointed out by Boden[25)] that the correlation time of reorientational jumps between equivalent sites (*e.g.* for *t*-butyl compounds it is the C_3'-rotation.) in the ordered phase of some plastic crystals tends to converge into the value of 5×10^{-9} s at the brittle-plastic phase transition. The deviation in the case of $(CH_3)_3CNO_2$ is probably related to the non-cubic structure in its Phase I.

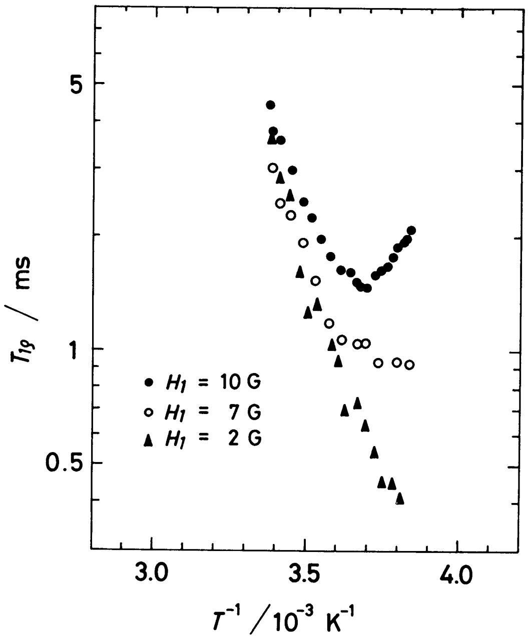

Fig. 5. Temperature dependence of the $T_{1\rho}$ (at 15 MHz) for three different rotating magnetic rf fields (H_1) in Phase I.

Relaxation in Phase I: In the plastic crystal phase, Phase I, the T_1 has a maximum which is frequency-dependent as can be seen in Fig. 3. On the low temperature side of this maximum the dominant relaxation mechanism is the overall molecular reorientation while the translational diffusion (self-diffusion) is responsible for the relaxation on the high temperature side as revealed by a study[26)] of the pressure dependence of the T_1. This assignment of motion was also put forward by Mazur and Nosel.[12)] When such two different relaxation mechanisms work, the experimental relaxation rate $1/T_{1\,\text{obsd}}$ can be written as

$$1/T_{1\,\text{obsd}} = 1/T_{1\,\text{trans}} + 1/T_{1\,\text{rot}}, \tag{9}$$

where $1/T_{1\,\text{trans}}$ and $1/T_{1\,\text{rot}}$ are the relaxation rate due to the translational diffusion and the overall molecular reorientation, respectively. According to Torrey's isotropic diffusion model,[27)]

$$1/T_{1\,\text{trans}} = 2.67\,\gamma^2\delta\langle\Delta H^2\rangle/\omega^2\tau, \tag{10}$$

when $\omega\tau\gg1$, where τ is the mean time between successive diffusional jumps and $\delta\langle\Delta H^2\rangle$ is the change in second moment due to the translational diffusion. The activation energy for the translational diffusion was determined to be 47±8 kJ mol^{-1} from the slope of the semilog plot of the $T_{1\,\text{trans}}$ against the inverse temperature. The temperature dependence of the $T_{1\rho}$ data at three different rotating rf fields is shown in Fig. 5. $T_{1\rho}$ measured at $H_1=10$ G assumes a minimum value of 1.50±0.05 ms at 271 K and $T_{1\rho}$ measured at 7 G shows a less obvious minimum 0.94±0.03 ms at 263 K. Isotropic diffusion model predicts that the minimum value of $T_{1\rho}$ is given by

$$1/T_{1\rho\,\text{minimum}} = 0.25\,\gamma^2\delta\langle\Delta H^2\rangle/\omega_1, \tag{11}$$

and on the high temperature side of the minimum, it is approximated by

$$1/T_{1\rho} = 0.5\,\gamma^2\delta\langle\Delta H^2\rangle\tau. \tag{12}$$

By substituting the experimental $T_{1\rho}$ minimum cited above and the appropriate value of $\omega_1=\gamma H_1$, $\delta<\Delta H^2>$ is estimated to be 1.0 ± 0.1 G^2 which agrees fairly well with the reduction of second moment 1.4 G^2 mentioned earlier. Activation parameters for the translational diffusion were determined by assuming the Arrhenius-type activation process (Eq. 8) for the correlation time τ and using $\delta<\Delta H^2>=1.0$ G^2 and are listed in Table 1. For this motion the result obtained from the $T_{1\rho}$ data is consistent with the result obtained from the T_1 data within the experimental error. The mean jump time at the melting point is about 6×10^{-7} s .

Relaxation in Liquid Phase: The T_1 in the liquid phase shows a monotonous increase on heating as shown in Fig. 3. The activation energy obtained from the slope of the T_1 was 9.7 ± 1.5 kJ mol^{-1} due to the translational motion (self-diffusion). Our result agreed with the result$^{7)}$ of NMR spin echo method for the self-diffusion ($E_a=10.8$ kJ mol^{-1}) in the liquid phase of $(CH_3)_3CNO_2$.

Discussion

The result of analysis of the nuclear magnetic relaxation is summarized in Table 1. In Phase II, the relaxation due probably to the overall molecular tumbling is also seen although it was not possible to derive a value of its activation energy. Whether or not the *t*-butyl reorientation is accompanied by the reorientation of the NO_2 group was difficult to determine by experiment.

The large electric dipole moment (12.35 C m) is responsible for the unique properties of 2-methyl-2-nitropropane among *t*-butyl compounds which form a plastic phase. The fact that the Phase I is not of cubic symmetry indicates that the molecular reorientation in this phase is not rapid enough to eliminate the effect of anisotropy of intermolecular forces.

Such an anisotropy in molecular interaction is even more prominent in Phase II, where the structure is reported to be triclinic.$^{3)}$ If the NO_2 group is also reorienting or even the molecule undergoes reorientation about its C_3 axis very vigorously, the molecule would assume on the average a cylindrical symmetry which would in turn lead to a crystal structure of higher symmetry.

These properties are probably related to the small value of the correlation time for *t*-butyl reorientation at $T_{\text{I-II}}$ as compared with many other plastic crystals. In other words, the molecular motion in 2-methyl-2-nitropropane is not as rapid as one would expect for a typical plastic crystal and as a result the lattice is a little harder.

The change in NMR properties at the III—II transition is much smaller than that at the II—I transition although the corresponding entropy changes are comparable (2.36*R* and 2.16*R*, respectively). The packing factor change is greater at $T_{\text{III-II}}$ than at $T_{\text{II-I}}$.$^{11)}$ To rationalize all these behaviors and even the existence of Phase II requires more elaborate studies including detailed crystal structures of all the solid phases.

References

1) A. H. McLellan, "Tables of Experimental Dipole Moments," Freeman, San Francisco (1963).

2) P. R. R. Langridge-Smith, R. Stevens, and A. P. Cox, *J. Chem. Soc., Faraday Trans. 2*, **76**, 330 (1980)

3) S. Urban, Z. Tomkowicz, J. Mayer, and T. Waluge, *Acta Phys. Pol.*, **A48**, 61 (1975).

4) R. W. Crowe and C. P. Smyth, *J. Am. Chem. Soc.*, **72**, 4009 (1950).

5) E. E. Toops, Jr., *J. Phys. Chem.*, **60**, 304 (1956).

6) C. Clemett and M. Davies, *Trans. Faraday Soc.*, **58**, 1705 (1962).

7) D. Kessler, A. Weiss, and H. Witte, *Ber. Bunsenges. Phys. Chem.*, **71**, 3 (1967).

8) R. Haffmans and I. W. Larkin, *J. Chem. Soc., Faraday Trans. 2*, **68**, 1729 (1972).

9) P. Freundlich, J. Kalenid, E. Narewski, and L. Soczyk, *Acta Phys. Pol.*, **A48**, 701 (1975).

10) S. Urban, *Acta Phys. Pol.*, **A49**, 741 (1976).

11) P. Freundlich and L. Sobczyk, *Mol. Cryst. Liq. Cryst.*, **65**, 197 (1981).

12) J. Mazur and W. Nosel, *Acta Phys. Pol.*, **A52**, 477 (1977).

13) J. Mayer, I. Natkaniec, and J. Sciesinski, *Acta Phys. Pol.*, **A52**, 665 (1977).

14) J. G. Powles and H. S. Gutowsky, *J. Chem. Phys.*, **21**, 1695 (1953).

15) H. Chihara, M. Otsuru, and S. Seki, *Bull. Chem. Soc. Jpn.*,**39**, 2145 (1966).

16) G. W. Smith, *J. Chem. Phys.*, **51**, 3569 (1969).

17) Y. Yukitoshi, H. Suga, S. Seki, and J. Itoh, *J. Phys. Soc. Jpn.*, **12**, 515 (1957).

18) G. W. Smith, *J. Chem. Phys.*, **54**, 174 (1971)

19) Z. M. El Saffer, J. Kalenik, and E. F. Meyer, *J. Chem. Phys.*, **56**, 1477 (1972).

20) D. E. Woessner, *J. Chem. Phys.*, **36**, 1 (1962).

21) S. Albert, H. S. Gutowsky, and J. A. Ripmeester, *J. Chem. Phys.*,**56**, 1332 (1972).

22) D. C. Look and I. J. Lowe, *J. Chem. Phys.*, **44**, 2995 (1966).

23) D. E. O'Reilly, E. M. Peterson, C. E. Scheie, and E. Seyfarth, *J. Chem. Phys.*, **59**, 3576 (1973).

24) P. S. Goyal, W. Nawrocik, S. Urban, J. Domoslawski, and I. Natkaniec, *Acta Phys. Pol.*, **A46**, 399 (1974).

25) N. Boden, *Chem. Phys. Lett.*, **46**, 141 (1977).

26) T. Hasebe and H. Chihara, unpublished.

27) H. C. Torrey, *Phys. Rev.*, **92**, 962 (1953); **96**, 690 (1954).